



澳門大學  
UNIVERSIDADE DE MACAU  
UNIVERSITY OF MACAU

# Outstanding Academic Papers by Students

## 學生優秀作品



DESIGN AND DEVELOPMENT OF AN EXPERIMENTAL  
APPARATUS FOR THE STUDY OF HEAT TRANSFER AND  
FRICTION FACTOR INSIDE THE MINI-TUBES WITH DIFFERENT  
INLET CONFIGURATIONS

by

**Leong Ngok Lam, David**

**D-B2-2728-0**

**U Kun Wai, Roy**

**D-B2-2775-4**

**B.Sc. in Electromechanical Engineering**

**2015/2016**



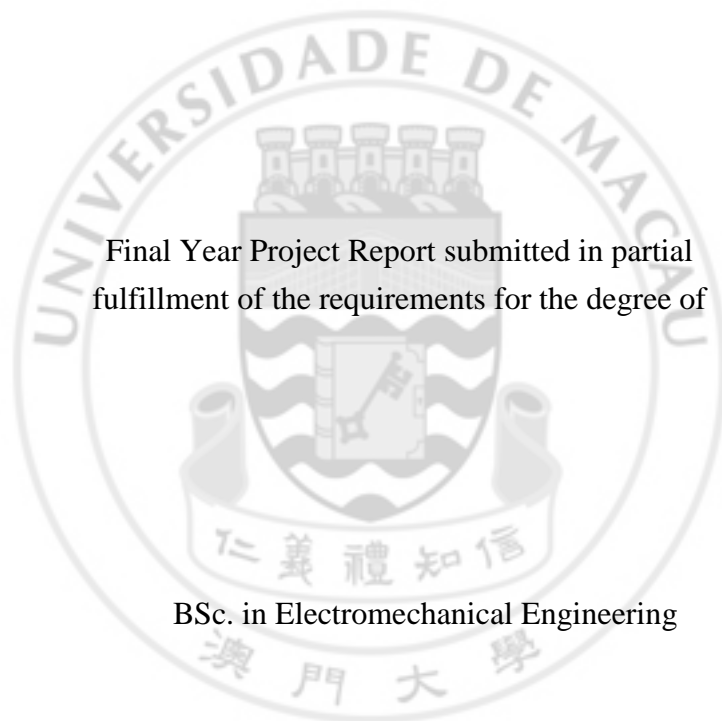
**Faculty of Science and Technology  
University of Macau**

Design and Development of an Experimental Apparatus for the Study of Heat Transfer  
and Friction Factor inside the Mini-Tubes with Different Inlet Configurations

by

Leong Ngok Lam (D-B2-2728-0)

U Kun Wai (D-B2-2775-4)



Final Year Project Report submitted in partial  
fulfillment of the requirements for the degree of

BSc. in Electromechanical Engineering

Faculty of Science and Technology  
University of Macau

2015/2016

University of Macau

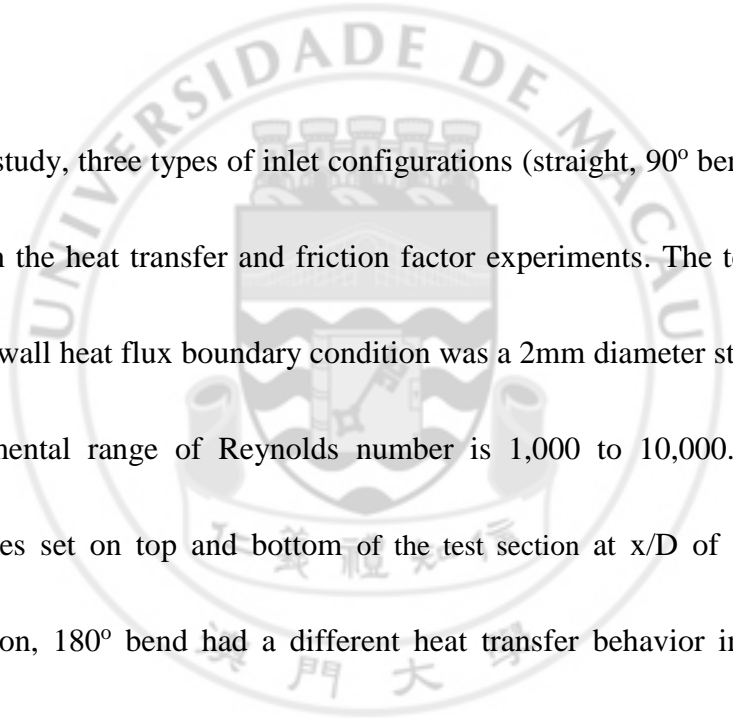
Abstract

Design and Development of an Experimental Apparatus for the Study of Heat Transfer  
and Friction Factor inside the Mini-Tubes with Different Inlet Configurations

by Leong Ngok Lam (D-B2-2728-0), U Kun Wai (D-B2-2775-4)

Project Supervisor

Prof. L.M. Tam



In this study, three types of inlet configurations (straight, 90° bend and 180° bend) were used in the heat transfer and friction factor experiments. The test section under the uniform wall heat flux boundary condition was a 2mm diameter stainless steel tube. The experimental range of Reynolds number is 1,000 to 10,000. There were 32 thermocouples set on top and bottom of the test section at  $x/D$  of 5 to 400. In the laminar region, 180° bend had a different heat transfer behavior in the developing region compared with others. However, in the transition region, different inlets have the similar heat transfer characteristics. The 180° bend has a higher turbulent heat transfer in the developed region. In the isothermal friction factor results, all the inlets are basically the same from the laminar to turbulent flow region.

## ACKNOWLEDGEMENT

We would like to thank to our supervisor, Professor L. M. Tam, for providing us with the knowledge from the lecture, and his supports during the preparation of this project. Furthermore, we would like to thank Dr. H. K. Tam and for his assistance, suggestions, also for providing us with the related materials to complete this project. Finally, we would like to thank the support from Institute of Development and Quality, Macau.



# TABLE OF CONTENT

TABLE OF CONTENT .....	I
LIST OF FIGURES .....	III
LIST OF TABLES .....	V
LIST OF ABBREVIATIONS .....	VI
CHAPTER 1: INTRODUCTION AND OBJECTIVES .....	1
1.1 LITERATURE REVIEW .....	2
1.2 OBJECTIVES .....	5
CHAPTER 2: EXPERIMENTAL SETUP .....	6
2.1 TEST SECTION ASSEMBLY .....	6
2.1.1 Inlet .....	9
2.1.2 Thermocouples and Required Equipment .....	11
2.1.3 DC Power Supply .....	14
2.2 FLUID DELIVERY SYSTEM .....	15
2.2.1 Test Fluid .....	15
2.2.2 High Pressure Nitrogen Tank .....	16
2.2.3 Pressure Vessel .....	16
2.2.4 Flow Controlling Valves .....	17
2.2.5 Receiving Tank and Submerge Pump .....	18
2.3 DATA ACQUISITION SYSTEM .....	18
2.3.1 Ni DAQ Chassis .....	18
2.3.2 Flow Meter .....	19
2.3.4 Pressure Transducer .....	20
2.3.5 Calibration .....	21
2.3.6 Computer Program .....	24

2.4	EXPERIMENTAL PROCEDURES .....	29
2.4.1	Preparation for the Test Section .....	30
2.4.2	Fill Test Fluid to the Pressure Vessel .....	30
2.4.3	Increase the Pressure in the Pressure Vessel .....	30
2.4.4	Pump the Test Fluid to the Test Section .....	30
2.4.5	Start the Experiment .....	31
	CHAPTER 3: VERIFICATION FOR THE EXPERIMENTAL SETUP .....	32
3.1	VERIFICATION FOR THE HEAT TRANSFER .....	32
3.2	VERIFICATION FOR THE ISOTHERMAL PRESSURE DROP .....	33
	CHAPTER 4: RESULTS AND DISCUSSION .....	35
4.1	RESULTS OF HEAT TRANSFER .....	35
4.2	RESULTS OF ISOTHERMAL FRICTION FACTOR .....	40
	CHAPTER 5: CONCLUSIONS .....	41
	CHAPTER 6: FUTURE WORKS .....	42
	REFERENCES .....	i
	APPENDIX (A): DATA OF FIGURE .....	ii
	APPENDIX (B): DATA REDUCTION .....	vi
	WORK BREAKDOWN .....	ix

## LIST OF FIGURES

<i>Number</i>	<i>Page</i>
Figure 1-1 Variation of local Nusselt number with length for three different inlet configurations in transition region .....	3
Figure 1-2 Ratio of local Nusselt number and terminal Nusselt number for different inlet configurations in turbulent flow [4] .....	3
Figure 1-3 Fully developed skin friction coefficients for three different inlet configurations in all flow regimes.....	4
Figure 1-4 Heat transfer for different inlet configurations in the transition region.....	4
Figure 2-1 Experimental setup for different inlet configurations: (a) straight, (b) 90° bend, (c)180° bend .....	7
Figure 2-2 High purity Dupont PFA .....	8
Figure 2-3 Arrangement of the thermocouples on the test section.....	9
Figure 2-4 Three types of inlet configurations in this study .....	10
Figure 2-5 Tube bender.....	10
Figure 2-6 Omega SA1XL-T .....	11
Figure 2-7 Omega TMQss-020U-6.....	11
Figure 2-8 Omega TJ36-CPSS-18U-12-CC.....	12
Figure 2-9 Omega bond 101 .....	12
Figure 2-10 Different types of fittings .....	13
Figure 2-11 Details of ferrule set .....	13
Figure 2-12 Rubber foam insulation roll.....	14
Figure 2-13 ZHAOZIN KXN-30100D DC power supply .....	14
Figure 2-14 FLUKE 376 AC/DC Clamp meter .....	15
Figure 2-15 FLUKE 17B digital multimeter.....	15
Figure 2-16 Test fluid .....	15
Figure 2-17 High pressure Nitrogen tank.....	16
Figure 2-18 Pressure regulating valve.....	16
Figure 2-19 High Pressure vessel.....	17
Figure 2-20 Two port valves .....	17
Figure 2-21 WALEY Screwed-Bonnet Needle Valve .....	17
Figure 2-22 Receiving tank.....	18



Figure 2-23 Submerged pump.....	18
Figure 2-24 SCXI 1000 Chassis.....	19
Figure 2-25 SCXI 1303 with two SCXI 1102Modules.....	19
Figure 2-26 Micro motion F series flow meter .....	20
Figure 2-27 Validyne DP15 pressure transducer .....	21
Figure 2-28 Validyne CD15 Carrier Demodulator .....	21
Figure 2-29 Pressure range chart of different diaphragms .....	21
Figure 2-30 Omega TMQss-020U-6 thermocouple probe and HCT-3030 constant temperature circulating bath.....	22
Figure 2-31 LabVIEW calibration interface .....	22
Figure 2-32 GE Druck PV211.....	23
Figure 2-33 User interface of LabVIEW .....	25
Figure 2-34 The interface of thermocouple in LabVIEW .....	26
Figure 2-35 User interface of MATLAB.....	27
Figure 2-36 Data reduction file generated by MATLAB.....	28
Figure 2-37 Data analysis report file by MATLAB .....	28
Figure 2-38 Data analysis report file by MATLAB.....	29
Figure 3-1 Comparison of the present heat transfer data at $x/D_i$ of 160 with experimental data of [3] at $x/D_i$ of 200.....	33
Figure 3-2 Friction factor characteristics for mini-tube under isothermal boundary condition...	34
Figure 4-1 Nusselt number for straight inlet in different flow regions .....	35
Figure 4-2 Nusselt number for 90° bend inlet in different flow regions .....	36
Figure 4-3 Nusselt number for 180° bend inlet in different flow regions .....	36
Figure 4-4 Nusselt number for different inlet configurations in laminar flow ( $Re=1,800$ ) .....	37
Figure 4-5 Nusselt number for different inlet configurations in transition flow ( $Re=4,000$ )...	37
Figure 4-6 Nusselt number for different inlet configurations in turbulent flow ( $Re=10,000$ ) .....	38
Figure 4-7 Nusselt number arrangement of bell-mouth inlet in transition flow .....	38
Figure 4-8 Heat transfer characteristics for three different inlet configurations at $x/D_i=160$ ..	39
Figure 4-9 Friction factor characteristics for three different inlet configurations under isothermal condition.....	40

## LIST OF TABLES

Table 2-1	Specifications of test section .....	8
-----------	--------------------------------------	---



## LIST OF ABBREVIATIONS

SYMBOL	DESCRIPTION	UNIT
$C_f$	friction factor coefficient	dimensionless
$c_p$	specific heat of the test fluid evaluated at $T_b$	J/(kg·K)
$D_i$	inside diameter of the test section (tube)	m
$D_o$	outside diameter of the test section (tube)	m
$f$	friction factor	dimensionless
$h$	fully developed peripheral heat transfer coefficient	W/(m <sup>2</sup> ·K)
$j$	Colburn-j factor [=St Pr <sup>0.67</sup> ]	dimensionless
$k$	thermal conductivity evaluated at $T_b$	W/(m·K)
$L$	length of the test section (tube)	m
$Nu$	local average or fully developed peripheral Nusselt number	dimensionless
$Pr$	local bulk Prandtl number	dimensionless
$Re$	local bulk Reynolds number	dimensionless
$T_b$	local bulk temperature of the test fluid	°C
$T_w$	local inside wall temperature	°C
$V$	average velocity in the test section	m/s
$x$	local axial distance along the test section from the inlet	m
$\Delta P$	pressure difference	Pa
$\mu_b$	absolute viscosity of the test fluid evaluated at $T_b$	Pa·s
$\mu_w$	absolute viscosity of the test fluid evaluated at $T_w$	Pa·s
$\rho$	density of the test fluid evaluated at $T_b$	kg/m <sup>3</sup>
TC	thermocouple	-

## CHAPTER 1: INTRODUCTION AND OBJECTIVES

In thermal engineering, the effect of inlet on heat transfer was necessary to be concerned for design a heat exchanger. Since the engineers wanted to develop the miniaturization of devices and components such as heat exchanger [1], the different types of heat transfer observations in mini- or even micro- tubes is indispensable. In the past studies, there was a few researches discussed the study of different inlet configurations [2] [3]. According to others research [4], different inlets of macro-tube had different heat transfer characteristics in developing region in steam-heated air flow experiment. However, there was lack experimental research discussing the heat transfer in mini-tubes with different inlet configurations. Therefore, design and develop an experiment in of heat transfer inside the mini-tubes with inlets in different angles is necessary. Besides, the friction factor is influenced with different inlet configurations [5], so the observation of friction factor in different inlet configuration has been done in this study.

## 1.1 LITERATURE REVIEW

Tam and Ghajar [2] had discussed the different effect of heat transfer in re-entrant, square-edged, bell-mouth three different inlet configurations. They had mentioned that the dip in the  $Nu-x/D_i$  curve was causing by the boundary layer along the tube wall is at first laminar and then changes through a transition region to the turbulent condition for the bell-mouth inlet. (Shown in Figure 1-1). In Boelter, Young and Iversen's steam-heated air flow experiment [4], had stated the difference in ratio of local Nusselt number and terminal Nusselt number of various inlet configurations in turbulent flow, as shown in Figure 1-2. It was shown that the local Nusselt number ratio of straight inlet was lower than 90° and 180° bend. Ghajar and Madon [5] had conducted an experiment about pressure drop measurements in the transition region. In Figure 1-3 was shown their results that presented the influence of friction factor in different inlet configurations on transition region. Ghajar and Tam [6] had done an experiment of the heat transfer measurements and correlations in the transition region for a circular tube with three different inlet configurations. It was stated that the influence of different inlets on heat transfer transition region, as shown in Figure 1-4, which the results will be discussed in data verification.

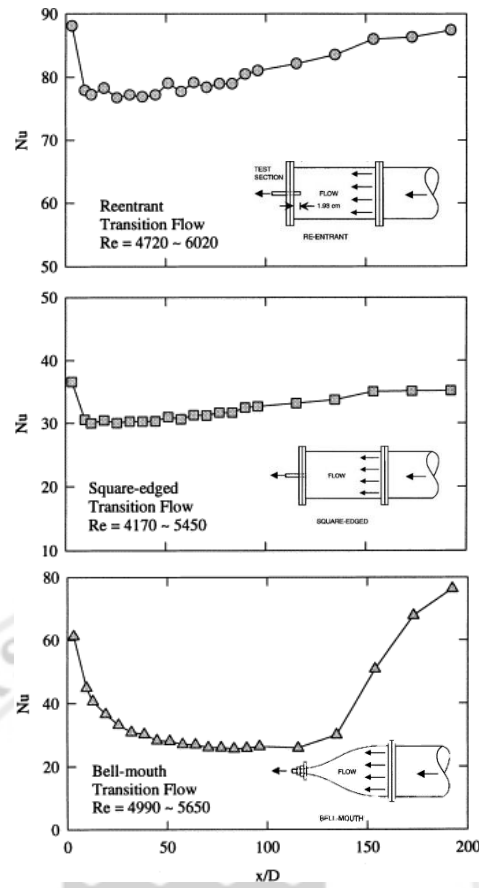


Figure 1-1 Variation of local Nusselt number with length for three different inlet configurations in transition region [2]

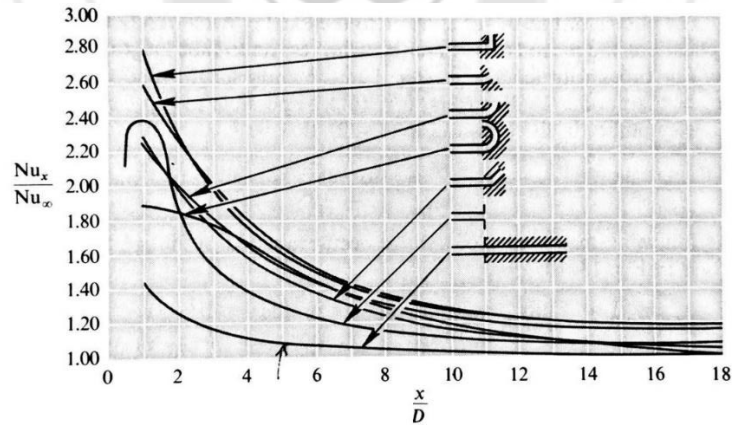


Figure 1-2 Measured local Nusselt numbers in the entry region of a circular tube for various entry configurations, air with constant surface temperature [4]

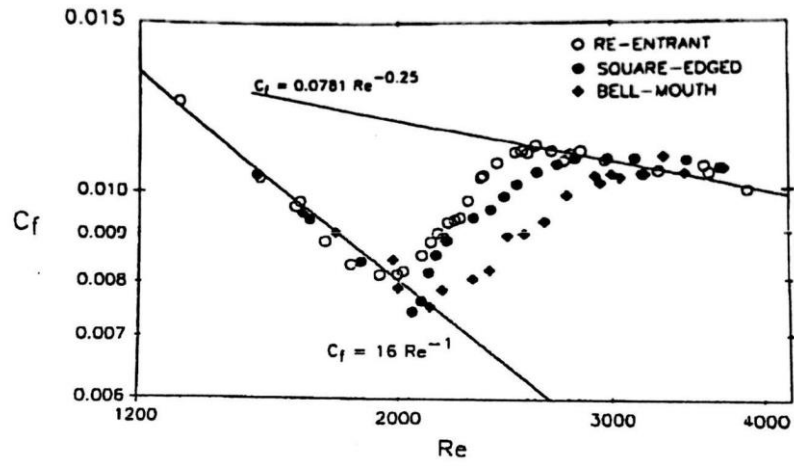


Figure 1-3 Fully developed skin friction coefficients for three different inlet configurations in all flow regimes [5]

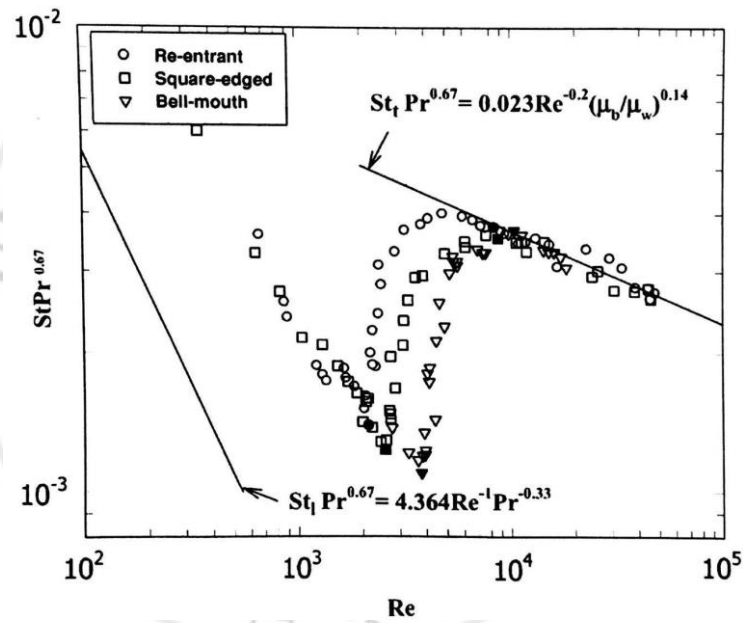


Figure 1-4 Heat transfer for different inlet configurations in the transition region [6]

## 1.2 OBJECTIVES

Based on the literature review, the heat transfer and friction factor of macro-tubes were affected by the inlet configurations. However, the effect of inlets on mini-tubes in heat transfer and friction factor was not investigated. Therefore, the objectives of this study are summarized below:

- i. Design and development of a simultaneous heat transfer and friction factor experimental setup for the horizontal mini-tube with different inlets (straight inlet, 90° bend, 180° bend).
- ii. Collect the experimental data and verify the reliability of the whole experimental system.
- iii. Analyze the effect of different inlets on heat transfer and friction factor in the entire flow regime.
- iv. Compare the heat transfer and friction factor of different inlets from developing to fully developed region

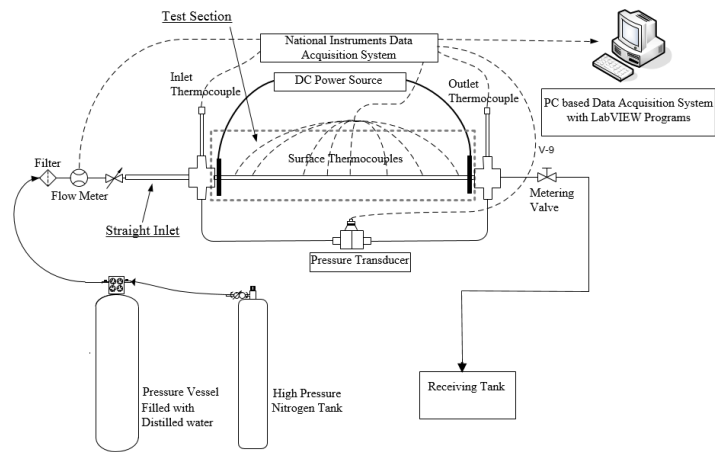


## CHAPTER 2: EXPERIMENTAL SETUP

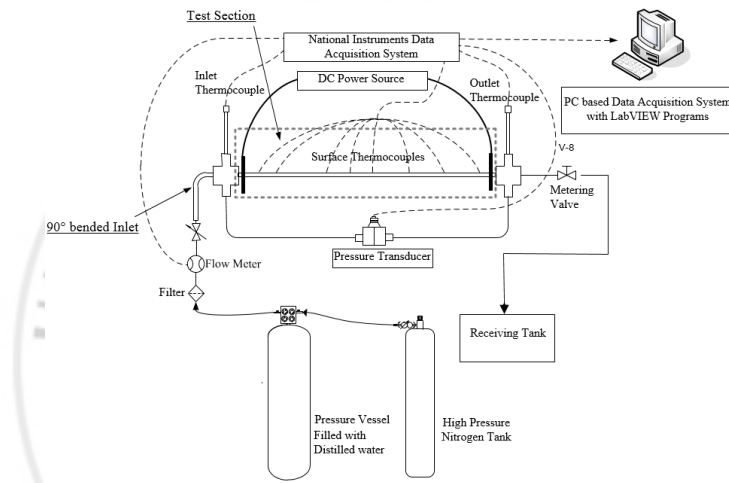
All friction factor and heat transfer experimental data used in this study were obtained from the experimental apparatus shown in Figure 2-1. In this Figure, the setups with three inlet configurations (straight, 90° bend and 180° bend) were installed before the test section. The experimental setup contain four components, named as test section assembly, fluid delivery system, data acquisition system, as also shown in Figure 2-1.

### 2.1 TEST SECTION ASSEMBLY

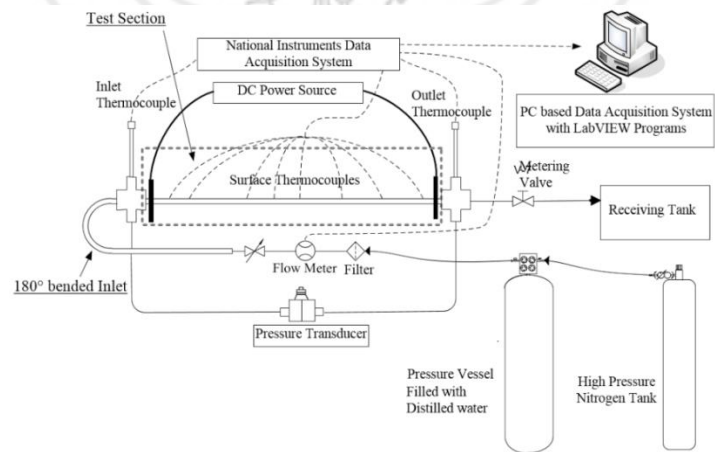
In this study, stainless steel tube was used as the test section and using different fittings to connect different parts of the test section. The test section was used copper wires to connect DC power supply. Copper wires were soldered on both sides of tube. The tube length between two soldered positions is the heating length. The specification of test section shows in Table 2-1. A pressure transducer was also connected to the inlet and outlet of the test section. High purity Dupont PFA (Figure 2-2) was connected on both sides of test section in order to be insulated current.



(a)



(b)



(c)

Figure 2-1 Experimental setup for different inlet configurations: (a) straight, (b) 90° bend, (c) 180° bend

Table 2-1 Specifications of test section

Inner diameter	Outer diameter	Total tube length	Heating length
(mm)	(mm)	(mm)	(mm)
2.0	3.1	955	900

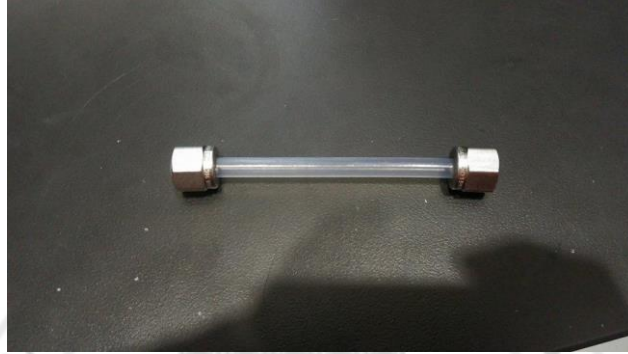


Figure 2-2 High purity Dupont PFA

Figure 2-3 shows the thermocouples (TC) denoted as TC1, TC2 were placed on top and bottom of the tube and the axial location on  $x/D_i = 5, 10, 20, 30, 40, 50, 60, 80, 100, 120, 140, 160, 200, 250, 300, 400$ . From the local peripheral wall temperature measurements at each axial location, the inside wall temperatures and local heat transfer coefficients were calculated by Ghajar and Kim [7]. In the present study, the experiment covered a local bulk Reynolds number range of 1,000 to 10,000 in laminar regions, a local bulk Nusselt number range of 5.1 to 121, a local bulk Prandtl number range of 5.4 to 6.4, inlet temperature and outlet temperature difference between  $5.5^{\circ}\text{C}$  to  $6.0^{\circ}\text{C}$  in turbulent and transition region,  $6.8^{\circ}\text{C}$  to  $7.0^{\circ}\text{C}$  in laminar region, and the heat balance errors within  $\pm 10\%$ .

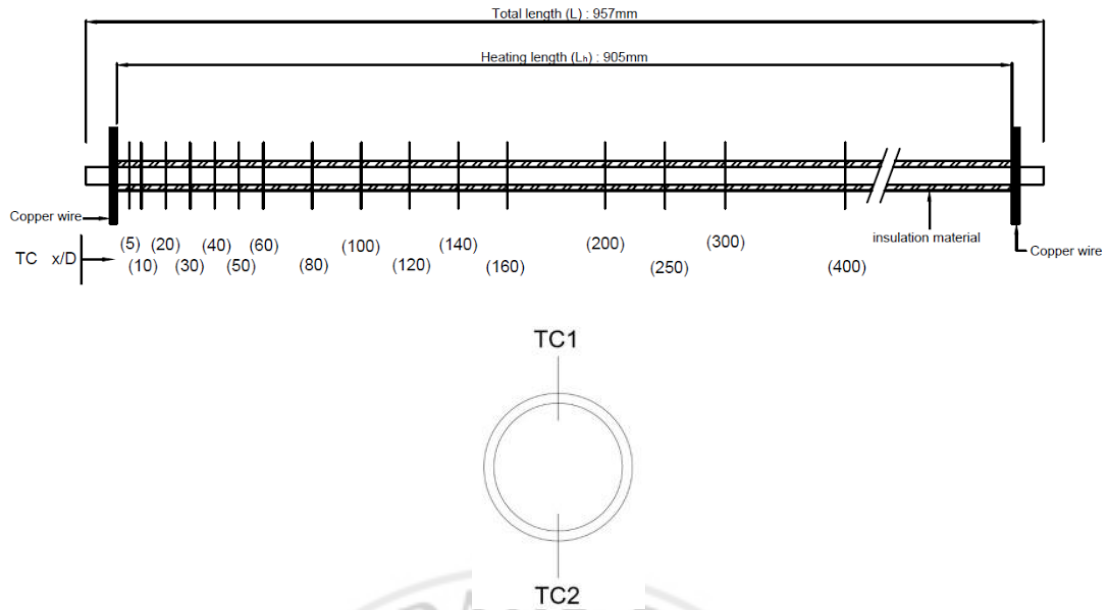


Figure 2-3 Arrangement of the thermocouples on the test section

### 2.1.1 Inlet

There are three types of inlet configurations in this study: straight, 90° and 180° bend, shown in Figure 2-4. The 90° and 180° bend inlet were made by bending the straight tube with a tube bender (Figure 2-5). The bending radius of the tube bender is 9/16 inch. A suitable wire was needed to put inside the tube before bending in order to ensure the tube will not be deformed during the bend.

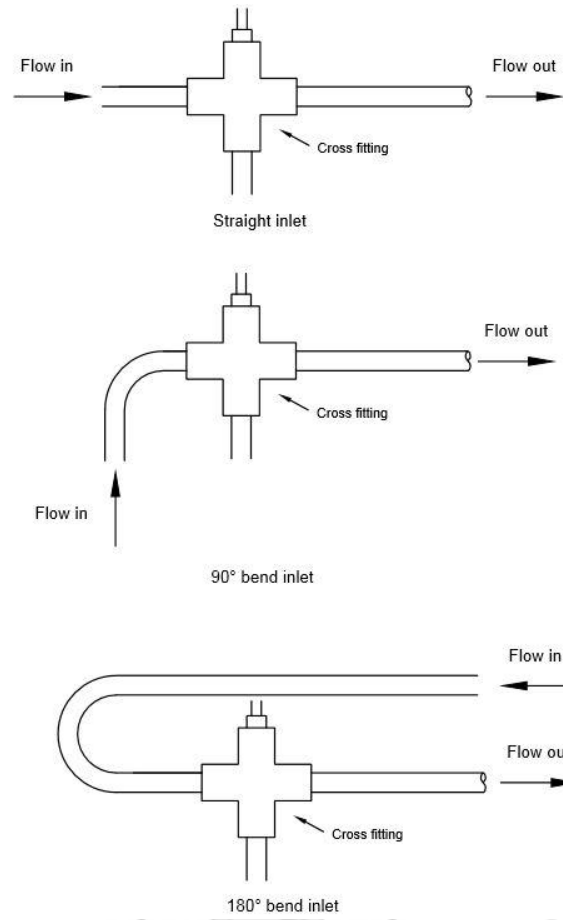


Figure 2-4 Three types of inlet configurations in this study



Figure 2-5 Tube bender

### 2.1.2 Thermocouples and Required Equipment

Thermocouples were used to measure the inlet, outlet and the surface of test section for the heat transfer experiment. There are three kinds of Type-T thermocouples used in this study.

- I. Self-adhesive thermocouple (SA1XL-T, Figure 2-6) was used to measure the upper and the bottom surface temperature of the test section.

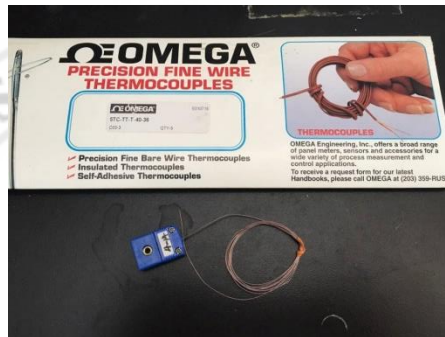


Figure 2-6 Omega SA1XL-T

- II. Thermocouple probe (TMQss-020U-6, Figure 2-7) was used to measure the inlet and outlet liquid temperature of the test section.



Figure 2-7 Omega TMQss-020U-6

III. Thermocouple probe (TJ36-CPSS-18U-12-CC, Figure 2-8) was used as a reference temperature for doing the calibration of other types of thermocouples and it have the calibration certificate from Omega Company.

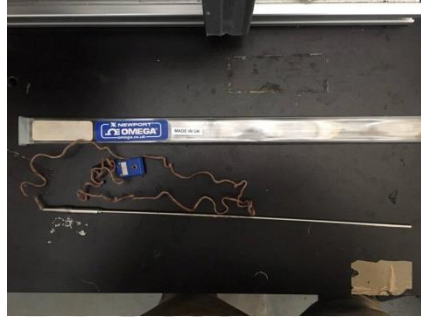


Figure 2-8 Omega TJ36-CPSS-18U-12-CC

In this study, the Omega bond 101 (Figure 2-9) was used to let the thermocouples place to the surface of the test section steady and safely. The Omega bond 101 is the mixture of the Thermally Conductive Epoxies and the Thermally Conductive Grease. The reason to choose this bond was it is thermally conductive, which is kept the conductivity to 105°C. It is also electrical insulated, tensile shear resistant and resist oils, solvents, most of acids. And the most important is it adheres to most surfaces.



Figure 2-9 Omega bond 101

To connect the flow meter, valves, test section and pressure transducer, just using tubes and pipes were not enough because they cannot connect each other themselves. The tube fittings were used to connect two or more tubes. And there were different types of tube fittings in order to connect tubes in different situation. In this study, union cross, 90° elbow union, straight union and straight union with two different tube outside diameter were used (see Figure 2-10). And all the connection of the fittings and the tubes were needed to use the ferrules (see Figure 2-11) which were used to avoid the leakage of test fluid from the fittings.



Figure 2-10 Different types of fittings

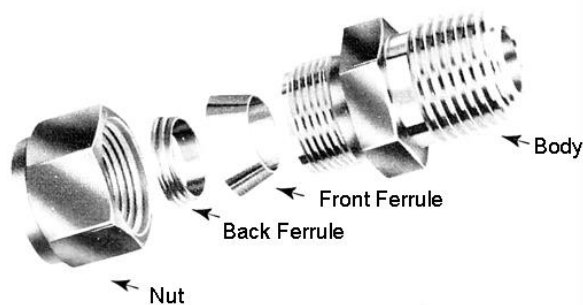


Figure 2-11 Details of ferrule set



The rubber foam insulation roll (Figure 2-12) was used as insulation material. It was placed on plastic sheet then covered at the top and bottom of the test section in order to avoid the heat release by air convection.



Figure 2-12 Rubber foam insulation roll

### 2.1.3 DC Power Supply

A ZHAOZIN KXN-30100D (Figure 2-13) DC power supply is used in this study to provide a uniform wall heat flux condition. Copper wires were used to connect the DC power supply to test section. The FLUKE 376 (Figure 2-14), AC/DC clamp meter, was used to measure the accurate current, and FLUKE 17B (Figure 2-15), Digital multimeter, was used to measure the accurate voltage.

In this experiment, the DC power supply is used to control the inlet and outlet temperature difference between  $5.5^{\circ}\text{C}$  to  $6.0^{\circ}\text{C}$  in turbulent and transition region,  $6.8^{\circ}\text{C}$  to  $7.0^{\circ}\text{C}$  in laminar region.



Figure 2-13 ZHAOZIN KXN-30100D DC power supply



Figure 2-14 FLUKE 376 AC/DC Clamp meter



Figure 2-15 FLUKE 17B digital multimeter

## 2.2 FLUID DELIVERY SYSTEM

The fluid delivery system is used to provide test fluid flow through the test section. The fluid delivery system includes high pressure nitrogen tank, high pressure vessel, flow controlling valves, receiving tank and submerge pump.

### 2.2.1 Test Fluid

According to the references, most of experiments were using water as the test fluid. Therefore, distilled water was used as test fluid in this experiment, as shown in Figure 2-16. The test fluid will re-pump to the high pressure vessel in order to reuse at most three times.



Figure 2-16 Test fluid

### 2.2.2 High Pressure Nitrogen Tank

The high pressure nitrogen tank (Figure 2-17) was the pressure source to push the test fluid to the test section. The reason to used nitrogen is that will not dissolvable in water and affect the fluid properties. A pressure regulating valve was connected with the tank shown in Figure 2-18. And the tank used in this study can contain  $9.3\text{m}^3$  and maximum 200 Bar gas in room temperature.



Figure 2-17 High pressure Nitrogen tank



Figure 2-18 Pressure regulating valve

### 2.2.3 Pressure Vessel

The pressure vessel was connected with the pressure regulating valve outlet to receive the nitrogen. The tank can bear a maximum pressure of 400psi and this experiment used 200psi to keep the test fluid flow through the test section at constant speed. This pressure vessel has four control valves which pressure inlet valve, high pressure water outlet valve, pressure release valve, water inlet valve. As shown in Figure 2-19.

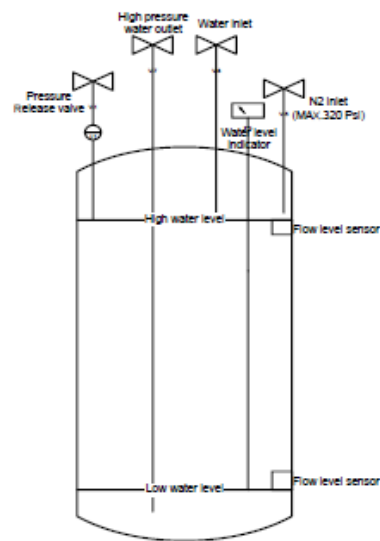


Figure 2-19 High Pressure vessel

#### 2.2.4 Flow Controlling Valves

There are two types of valves in this experiment. The two port valves (Figure 2-20) can start and stop the flow immediately. The WALEY Stainless Steel Screwed-Bonnet Needle Valve (Figure 2-21) can control the accurate flow rate.



Figure 2-20 Two port valves



Figure 2-21 WALEY Screwed-Bonnet Needle Valve

### 2.2.5 Receiving Tank and Submerge Pump

This experiment is an open loop system, after the test fluid flow through the test section, it flows into the receiving tank (Figure 2-22). And the test fluid is pumped back to the high pressure vessel by using submerged pump (Figure 2-23) after the pressure inside the vessel is released.



Figure 2-22 Receiving tank



Figure 2-23 Submerged pump

## 2.3 DATA ACQUISITION SYSTEM

The National Instruments Data Acquisition System was used to record and store the data measured in this study. All the data such as the temperatures measured by the thermocouples, the pressure difference measured by the pressure transducer and the flow rate measured by the flow meter were recorded and stored by this system.

### 2.3.1 Ni DAQ Chassis

An AC powered four-slot SCXI 1000 chassis (Figure 2-24) serves signal conditioning, supplying power and control circuitry. In this study two SCXI 1303



32-Channel Isothermal Terminal Blocks were connected to two SCXI 1102 Modules, shown in Figure 2-25. SCXI 1000 chassis have a high accuracy thermistor, cold-junction temperature sensor and an isothermal copper plane to minimize the temperature gradient across the screw terminals, which are used to attach the blocks to the terminals. The signals from flow meter, thermocouples, pressure transducer are connected to the screw terminals inside the SCXI 1303 Block, which are used to attach the blocks to the terminals, and transfer to computer programmer LabVIEW to record and store the data.



Figure 2-24 SCXI 1000 Chassis



Figure 2-25 SCXI 1303 with two SCXI 1102 Modules

### 2.3.2 Flow Meter

Micro motion F series flow meter (Figure 2-26) was used to measure flow rate in this study. The Micro motion F series flow meter was calibrated by the manufacturer. The accuracy of the mass flow rate is within  $\pm 1.75\%$ . Flow meter was connected to the

NI SCXI 1303 to record flow rate, which using in computer programmer LabVIEW.

The flow rate shown in the display of the meter was chosen for reference to tuning the reading in the LabVIEW program



Figure 2-26 Micro motion F series flow meter

#### 2.3.4 Pressure Transducer

In this study, Validyne DP15 pressure transducer (Figure 2-27) was used to measure the pressure difference between two input pressure and give out a voltage signal by CD15 Carrier Demodulator (Figure 2-28). And the range of the voltage signal provided by the Demodulator was  $\pm 10$  Vdc. The two inputs of this transducer were connected with the inlet and outlet of the test section by pipes and fittings. There were different diaphragms required to measure the different range of the pressure difference precisely (Figure 2-29).

This study was chosen No. 36 and 44 diaphragms which the pressure range was between 0 to 35kPa and 0 to 220kPa, where No. 36 was for laminar and transition regions, No. 44 for transition and turbulent region.



Figure 2-27 Validyne DP15 pressure transducer      Figure 2-28 Validyne CD15 Carrier Demodulator

PRESSURE RANGE CHART						
Range Dash No.	PSI	IN HG.	IN H <sub>2</sub> O	KPA	TORR	CM H <sub>2</sub> O
20	.125	.25	3.5	.86	6.5	8.80
22	.20	.41	5.5	1.40	10.3	14.0
24	.32	.65	8.9	2.2	16.5	22.5
26	.50	1.02	14.0	3.5	25.8	35.0
28	.80	1.6	22.2	5.5	41.4	56.0
30	1.25	2.5	35.0	8.6	65.0	88.0
32	2.0	4.1	55.0	14.0	103	140
34	3.2	6.5	90	22.0	165	225
36	5.0	10.2	140	35.0	258	350
38	8.0	16.0	222	55.0	414	560
40	12.5	25.0	350	86.0	650	880
42	20	41.0	550	140	1030	1400
44	32	65.0	890	220	1650	2250
46	50	102	1400	350	2580	3500
48	80	160	2220	550	4140	5600
50	125	250	3500	860	6500	8800
52	200	410	5500	1400	10300	14000
54	320	650	8900	2200	16500	22500
56	500	1020	14000	3500	25800	35000
58	800	1600	22200	5500	41400	56000
60	1250	2500	35000	8600	65000	88000
62	2000	4100	55000	14000	103000	140000
64	3200	6500	89000	22000	165000	225000

Figure 2-29 Pressure range chart of different diaphragms

### 2.3.5 Calibration

In this study, thermocouples and pressure transducer were required to be calibrated before the experiment in order to ensure the accuracy. And there the methods of calibration of thermocouples and pressure transducer stated below:

#### 2.3.5.1 Thermocouple Calibration

The Omega TMQss-020U-6 thermocouple probe (Figure 2-30) is used to calibrate the thermocouples. This probe is used with a HCT-3030 constant temperature circulating bath (Figure 2-30) for calibration. As the working range of the thermocouples is 15°C



to 60°C, the calibration data was taken each 5°C from 15°C to 60°C. The calibrating data was processed in LabVIEW program, by creating a linear equation of each thermocouple. After calibration a calibration report can be generated by the LabVIEW program to prove those thermocouples have been calibrated shown as Figure 2-31.

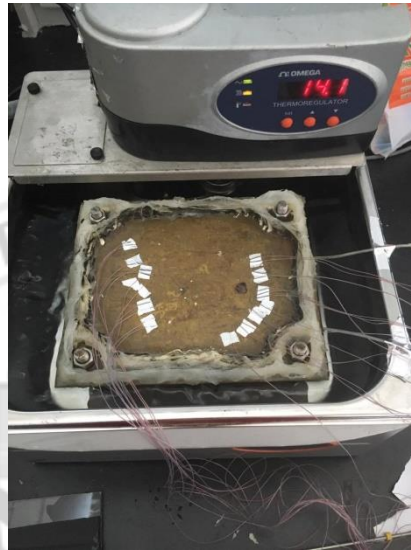


Figure 2-30 Omega TMQss-020U-6 thermocouple probe and HCT-3030 constant temperature circulating bath

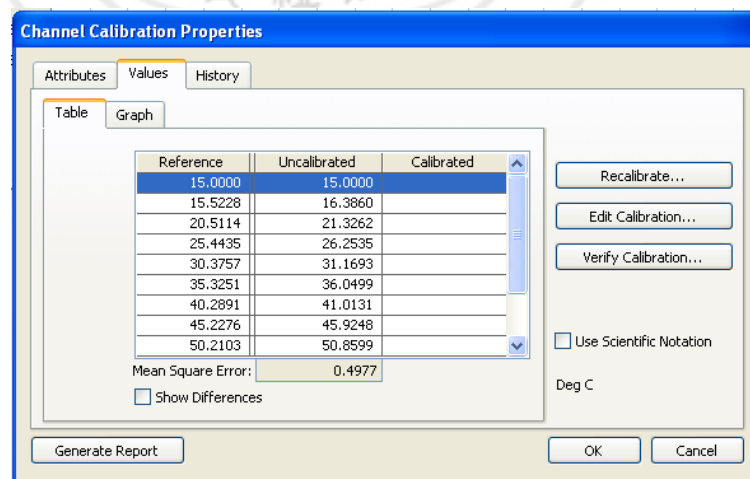


Figure 2-31 LabVIEW calibration interface

### 2.3.5.2 Pressure Transducer Calibration

To calibrate the pressure transducer, a pneumatic pressure and vacuum pump is needed and GE Druck PV211 (Figure 2-32) was used in this study. The pressure range that the pump can generate is 0 to 600 psi. And the calibration needs to be finished with the LabVIEW which can display the voltage signal of the pressure transducer.



Figure 2-32 GE Druck PV211

First, connect the pressure transducer and the hose of the pump, then close the pressure release valve. Before pressing the handles, there was no pressure added to the pressure transducer so the voltage in LabVIEW should be zero so that tuned the “zero” switch of the demodulator to make the reading of the voltage in LabVIEW be 0V.

Then press the handle of the pump to create a maximum operational pressure of the diaphragm. At that time the voltage reading of LabVIEW may not be the full scale voltage (10V), so tune the “span” switch to make the reading be 10V.

This process must be done at least three times in order to reduce the voltage reading of the zero pressure to 0.001V.

#### 2.3.6 Computer Program

In this study, LabVIEW (Laboratory Virtual Instrumentation Engineering Workbench) and MATLAB (Matrix Laboratory) were the mainly computer programs used to collect and analysis the experimental data. By connecting NI DAQ Device (National Instruments Data acquisition Device) and computer to record the experimental data by LabVIEW, the data was acquired, analyzed and presented by MATLAB.

##### 2.3.6.1 Labview Program

LabVIEW was used to record and analysis experimental data, besides it also presented the experimental condition and calibration equipment. LabVIEW received the temperatures, pressure drop and flow rate from the sensors by using data acquisition system.

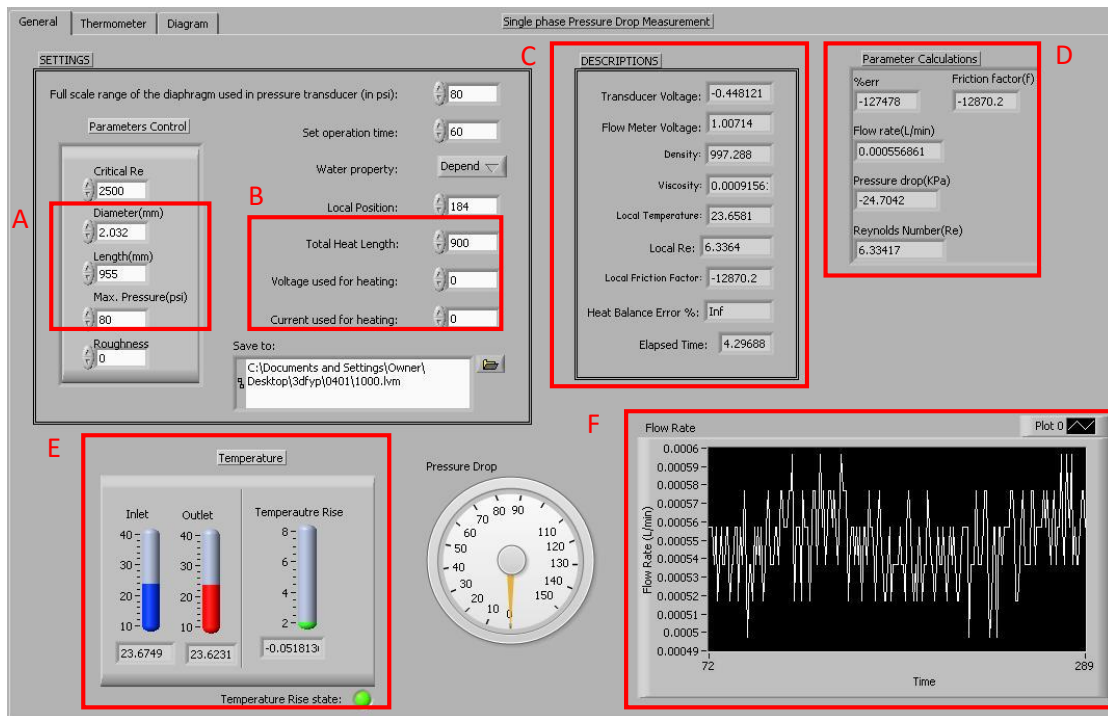


Figure 2-33 User interface of LabVIEW

In the Figure, red box A to F was used to analysis the whole experimental condition.

A: Parameters control. Input the diameter of the testing pipe, length of the testing pipe and maximum pressure of the diaphragm used to measure in the experiment. The maximum pressure of the diaphragm used in this experiment were 8psi and 220psi for laminar and turbulence flow.

B: Settings. Input the heating length of the testing section, voltage and current used for heating. In this experiment, the heating length was set to 900mm. Voltage and current needed to input during the experiment.

C: Descriptions of various variables. Mainly focus on the heat balance error and it was within  $\pm 10\%$  during the experimental process.

D: Parameters monitoring. Friction factor, flow rate, pressure drop and Reynolds number were presented in here.

E: Inlet temperature, outlet temperature and difference between the inlet and outlet temperature. In this experiment, inlet and outlet temperature were needed to be control in different between  $5.5^{\circ}\text{C}$  to  $6.0^{\circ}\text{C}$ .

F: Flow rate monitor. Ensure and monitor the stability of the flow rate.

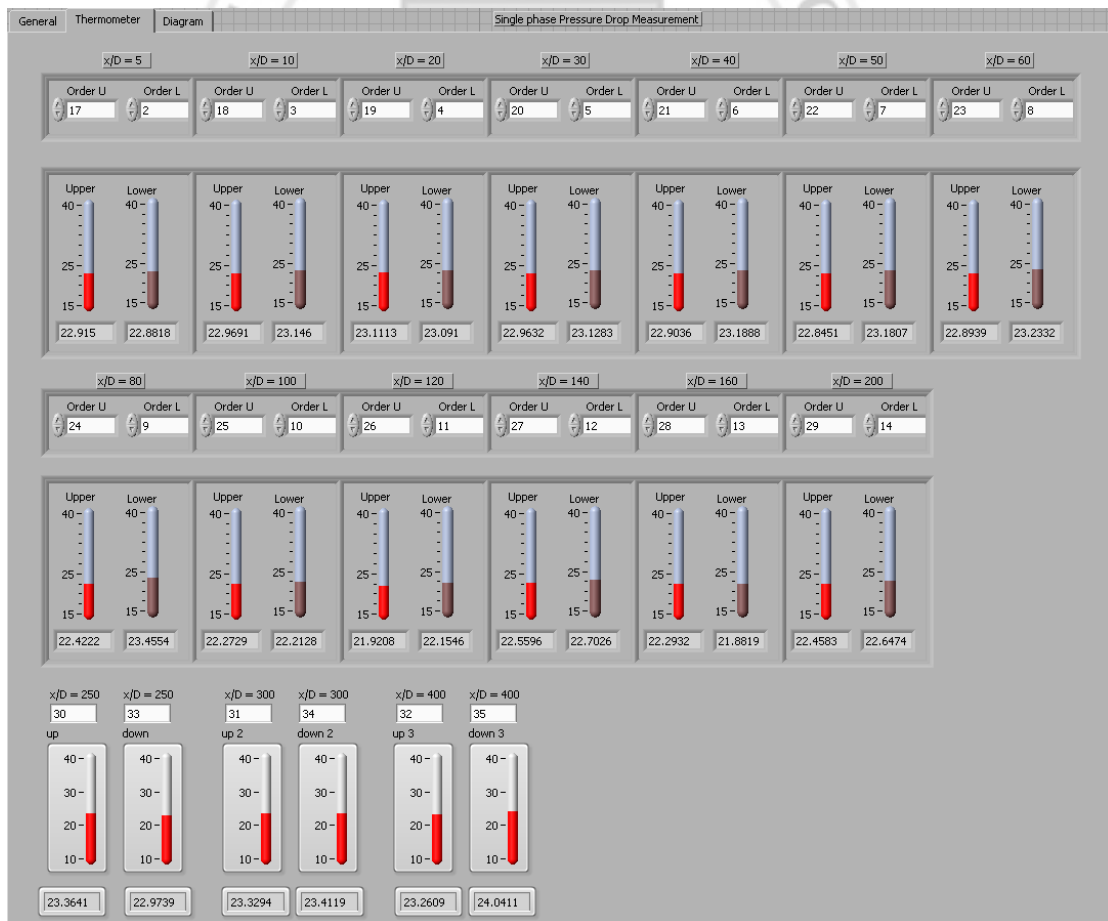


Figure 2-34 The interface of thermocouple in LabVIEW



Import - D:\Matlab\bin\3dtyp\_CopyResult\calibration\_0.xls

IMPORT VIEW

Range: D2:B27

Column selection: ☐ Replace ☐ Unimportable cells with: NaN

Variable Names Row: 1

Cell Array

Import Selection

calibration\_0.xls

FileDate	FileDate	RunNumber	Re	InletTemp	OutletTemp	Flowrate	Current	Voltage	RoomTemp	f1	P1	kPa1	T1up	T1down	T2up	T2down	T3up	T3down	T4up	T4down	T5up	T5down
2016/04/08	10000.lvm	10000.txt	1.003e+03	29.4307	31.1310	0.0817	15.0000	2.8400	27.4947	0.2016	8.3319	8.3319	26.6792	26.2578	26.7107	26.9476	27.0910	27.1148	27.4480	27.4947	27.8066	27.8066
3016/04/08	10000.lvm	1200.txt	1.2070e+03	29.4477	31.8644	0.0971	17.7000	3.1400	28.1551	0.1472	8.5763	8.5763	27.3071	26.8814	27.2930	27.3335	27.7378	27.7018	28.2038	28.1551	28.6919	28.6919
4016/04/08	12000.lvm	1400.txt	1.4096e+03	29.4368	31.8986	0.1133	19	3.3600	28.2640	0.1119	8.8996	8.8996	27.3453	26.9117	27.2798	27.2476	27.7689	27.7270	28.3070	28.2640	28.8647	28.8647
5016/04/08	14000.lvm	1600.txt	1.6040e+03	29.4235	30.9990	0.1302	18.1000	3.2200	27.0519	0.0889	9.3223	9.3223	26.3435	25.9491	26.3297	26.2421	26.6305	26.5308	26.9625	27.0519	27.3893	27.3893
6016/04/08	16000.lvm	1800.txt	1.8071e+03	29.4126	31.1990	0.1464	18.9000	3.3200	26.0096	0.0736	9.7557	9.7557	26.0300	25.7113	26.0851	25.9714	26.2734	26.1409	26.5540	26.6096	26.9311	26.9311
7016/04/08	18000.lvm	2000.txt	2.0042e+03	29.4033	29.9378	0.1663	20.4000	3.5000	26.4143	0.0614	10.4981	10.4981	25.8006	25.5776	25.9127	25.8031	26.0685	25.9626	26.3787	26.4143	26.6940	26.6940
8016/04/08	20000.lvm	2100.txt	2.1166e+03	29.4023	29.0066	0.1757	20.4000	3.5800	26.3464	0.0588	11.2209	11.2209	25.7433	25.5478	25.8650	25.7523	26.0067	25.9134	26.3185	26.3464	26.5923	26.5923
9016/04/08	21000.lvm	2200.txt	2.2054e+03	29.4133	29.4271	0.1822	21.7000	3.7500	26.5709	0.0577	11.8507	11.8507	25.9958	25.8069	26.0809	25.9437	26.2146	26.1171	26.5762	26.5709	26.8607	26.8607
10016/04/08	22000.lvm	2300.txt	2.3107e+03	29.4229	29.6412	0.1904	22.5000	3.9300	26.6641	0.0571	12.8011	12.8011	26.1196	25.9120	26.1812	26.0287	26.3042	26.2110	26.8884	26.6641	26.9446	26.9446
11016/04/08	23000.lvm	2400.txt	2.4196e+03	29.4176	29.9973	0.1981	23.7000	4.0900	26.6294	0.0560	13.5987	13.5987	26.2924	26.0889	26.3276	26.1831	26.4448	26.3655	26.8555	26.8294	27.1028	27.1028
12016/04/08	24000.lvm	2500.txt	2.5052e+03	29.4180	29.7415	0.2062	23.7000	4.0900	26.6941	0.0544	14.3106	14.3106	26.1906	26.0033	26.2174	26.0657	26.3287	26.2945	26.7945	26.6941	26.9074	26.9074
13016/04/08	25000.lvm	2600.txt	2.6156e+03	29.4232	29.2427	0.2165	23.2000	4.0200	26.4452	0.0524	15.1848	15.1848	25.9746	25.8025	26.0117	25.8878	26.1233	26.0743	26.4316	26.4452	26.5748	26.5748
14016/04/08	26000.lvm	2700.txt	2.7055e+03	29.4212	29.4914	0.2233	24.1000	4.1800	26.5662	0.0511	15.7706	15.7706	26.1099	25.9526	26.1179	25.9946	26.2361	26.1973	26.5444	26.5662	26.7122	26.7122
15016/04/08	27000.lvm	2800.txt	2.8037e+03	29.4304	29.6382	0.2310	24.8000	4.2900	26.6352	0.0499	16.4594	16.4594	26.2096	26.0489	26.1870	26.0645	26.3153	26.2793	26.6038	26.6352	26.7959	26.7959
16016/04/08	28000.lvm	2900.txt	2.9130e+03	29.4259	29.4331	0.2406	24.9000	4.3000	26.5295	0.0484	17.3242	17.3242	26.1318	25.9782	26.1056	26.0087	26.2353	26.2119	26.4779	26.5295	26.6812	26.6812
17016/04/08	29000.lvm	3000.txt	3.0064e+03	29.4276	29.5194	0.2481	25.5000	4.3800	26.5147	0.0474	18.0243	18.0243	26.1971	26.0447	26.1122	26.0566	26.2810	26.2665	26.5099	26.5747	26.7451	26.7451
18016/04/08	30000.lvm	3100.txt	3.1108e+03	29.4303	29.5451	0.2731	26.9000	4.6100	26.5839	0.0443	20.5354	20.5354	26.2777	26.1672	26.1824	26.1233	26.3246	26.3337	26.4966	26.5839	26.8196	26.8196
19016/04/08	31000.lvm	3200.txt	3.6080e+03	29.4297	29.4556	0.2979	27.8000	4.7800	26.5611	0.0424	23.2477	23.2477	26.3557	26.2797	26.2151	26.1592	26.3303	26.3607	26.4433	26.5611	26.8407	26.8407
20016/04/08	36000.lvm	4000.txt	4.0134e+03	29.4305	29.4073	0.3315	29.1000	4.9800	26.5610	0.0402	27.3582	27.3582	26.3891	26.3413	26.2998	26.2223	26.3041	26.4010	26.4356	26.5610	26.8966	26.8966
21016/04/08	40000.lvm	4500.txt	4.5090e+03	29.4275	29.2575	0.3731	30.8000	5.2100	26.5158	0.0384	33.0692	33.0692	26.3571	26.4211	26.2541	26.2361	26.3912	26.3912	26.5156	26.8778	26.8778	26.8778
22016/04/08	45000.lvm	5000.txt	5.0072e+03	29.4304	29.5610	0.4129	33.1000	5.5900	26.7130	0.0372	39.2628	39.2628	26.6174	26.7046	26.4787	26.4572	26.4868	26.5989	26.5989	26.7130	27.1603	27.1603
23016/04/08	50000.lvm	5500.txt	5.5087e+03	29.4309	29.2709	0.4537	34.1000	5.7900	26.8397	0.0363	46.6710	46.6710	26.5827	26.7177	26.4467	26.4462	26.4201	26.5441	26.5358	26.6397	27.0792	27.0792
24016/04/08	55000.lvm	6000.txt	6.0030e+03	29.4389	29.2296	0.4966	35.4000	5.9400	26.6927	0.0357	54.5168	54.5168	26.6874	26.7905	26.5926	26.5214	26.4994	26.5947	26.5928	26.6927	27.1521	27.1521
25016/04/08	60000.lvm	7000.txt	7.0153e+03	29.4485	29.1853	0.5808	38.1000	6.3700	26.8096	0.0350	73.0660	73.0660	26.8626	27.0073	26.7093	26.6970	26.6970	26.7093	26.7093	26.8096	27.3237	27.3237
26016/04/08	70000.lvm	8000.txt	8.0042e+03	29.4628	29.4123	0.6609	41.5000	6.8900	27.0831	0.0347	145.9351	145.9351	27.5086	27.7816	27.3412	27.2201	26.9663	27.0783	27.2018	27.2206	27.6923	27.6923
27016/04/08	100000.lvm	10000.txt	1.0010e+04	29.4890	29.1322	0.8289	45.6000	7.4900	27.2206	0.0343	145.9351	145.9351	27.5086	27.7816	27.3412	27.2201	26.9663	27.0783	27.2018	27.2206	27.6923	27.6923

Figure 2-36 Data reduction file generated by MATLAB

Plot - Notepad

File Edit Format View Help

Exp date: 05/04/16

Generate date: 27/04/16

Inner diameter: 0.0800

Outer diameter: 0.1250

Heating length: 35.4331

Run	x/D	Tbulk	Re	Nu	Pr	Gr	mub/muw	ht/hb	havg
1000	5.00	74.23	936.27	7.62	6.40	53.78	1.0539	1.0000	398
1200	5.00	74.16	1114.81	8.20	6.40	54.05	1.0544	1.0000	428
1400	5.00	74.12	1289.31	9.11	6.41	56.60	1.0571	1.0000	476
1600	5.00	74.12	1477.18	11.18	6.41	56.31	1.0568	1.0000	584
1800	5.00	74.10	1655.97	13.82	6.41	49.14	1.0496	1.0000	722
2000	5.00	74.04	1876.55	16.51	6.42	46.01	1.0465	1.0000	862
2100	5.00	74.02	1965.48	17.17	6.42	48.78	1.0494	1.0000	897
2200	5.00	74.00	2067.46	18.39	6.42	47.30	1.0480	1.0000	961
2300	5.00	73.99	2169.41	19.34	6.42	45.80	1.0465	1.0000	1010
2400	5.00	73.98	2254.38	19.94	6.42	46.09	1.0468	1.0000	1042
2500	5.00	73.97	2343.57	20.81	6.42	46.20	1.0469	1.0000	1087
2600	5.00	73.97	2445.82	21.66	6.42	46.00	1.0467	1.0000	1131
2700	5.00	73.95	2538.95	22.30	6.42	47.04	1.0478	1.0000	1165
2800	5.00	73.94	2628.05	22.95	6.43	46.87	1.0477	1.0000	1199
2900	5.00	73.93	2729.95	23.79	6.43	47.54	1.0484	1.0000	1243
3000	5.00	73.93	2815.15	24.77	6.43	47.96	1.0488	1.0000	1294
3300	5.00	73.92	3104.30	27.23	6.43	47.58	1.0485	1.0000	1422
3600	5.00	73.91	3389.16	29.45	6.43	47.79	1.0487	1.0000	1539
4000	5.00	73.90	3763.41	32.47	6.43	48.98	1.0500	1.0000	1696
4500	5.00	73.87	4225.73	35.66	6.43	49.33	1.0504	1.0000	1863
5000	5.00	73.87	4684.95	38.72	6.43	52.00	1.0532	1.0000	2022
5500	5.00	73.84	5155.83	41.04	6.43	52.73	1.0540	1.0000	2143
6000	5.00	73.85	5619.72	43.72	6.43	55.31	1.0567	1.0000	2284
7000	5.00	73.82	6561.57	47.76	6.44	58.60	1.0602	1.0000	2495
8000	5.00	73.80	7500.32	52.26	6.44	60.81	1.0625	1.0000	2730
9914	5.00	73.78	9377.13	59.23	6.44	65.92	1.0679	1.0000	3093

Figure 2-37 Data analysis report file by MATLAB



*-----*										
RUN NUMBER 1000										
*-----*										
	x/D	Tbulk	Re	Pr	Nu	Gr	mub/muw	ht/hb	havg	
1	5.00	70.36	939.24	6.77	13.16	33.32	1.0417	0.5192	684	0.007452
2	10.00	70.48	940.74	6.76	11.83	37.31	1.0464	0.8370	615	0.006691
3	20.00	70.72	943.74	6.74	10.16	43.97	1.0540	0.9418	529	0.005739
4	30.00	70.96	946.75	6.71	8.09	55.94	1.0679	0.4206	421	0.004561
5	40.00	71.20	949.76	6.69	9.07	50.53	1.0604	0.7499	472	0.005100
6	50.00	71.44	952.77	6.66	8.30	55.90	1.0659	0.9060	432	0.004658
7	60.00	71.68	955.79	6.64	8.07	58.21	1.0677	0.8324	420	0.004519
8	80.00	72.16	961.84	6.59	7.94	60.60	1.0685	0.5981	414	0.004429
9	100.00	72.64	967.90	6.55	8.02	61.39	1.0675	0.6468	418	0.004459
10	120.00	73.11	973.98	6.50	9.16	55.04	1.0588	0.1758	478	0.005070
11	140.00	73.59	980.08	6.46	6.79	76.14	1.0794	0.9224	354	0.003741
12	160.00	74.07	986.19	6.41	7.45	70.96	1.0719	0.5690	389	0.004090
13	200.00	75.03	998.45	6.32	7.46	74.17	1.0712	1.1330	390	0.004063

Figure 2-38 Data analysis report file by MATLAB

## 2.4 EXPERIMENTAL PROCEDURES

In this study, the experiment was performed with a 316-stainless steel straight smooth tube and parts of different angle inlet which are also made by 316-stainless steel. And distilled water is the working fluid. The procedure of heat transfer measurements and isothermal pressure drop is similar, just a heating process needs to be done in heat transfer measurements which the isothermal pressure drop do not need. The experiments involve 5 major steps.

Step 1: preparation for the test section

Step 2: fill test fluid to the pressure vessel

Step 3: increase the pressure in the pressure vessel

Step 4: pump the test fluid to the test section

Step 5: start the experiment



#### 2.4.1 Preparation for the Test Section

The preparation for the test section is included the experiment setup, the devices and the calibration of them, and the computer programs.

#### 2.4.2 Fill Test Fluid to the Pressure Vessel

First switch on the valves of “test fluid input” and “gas release” on the pressure vessel, then turn on the electronic pump to pump the test fluid into the vessel from receiving tank. Even the test fluid is fresh from the distilled water bottle we still flow them to receiving tank to convenient the pump work. There is 6 Liters of distilled water pumped into the pressure vessel for the experiment run.

#### 2.4.3 Increase the Pressure in the Pressure Vessel

Switch on the main valve of the nitrogen tank and the “gas input” valve of the pressure vessel; make sure other valves on the pressure vessel are closed. Then tune the pressure regulating valve to release the nitrogen into the pressure vessel until the inside pressure of the pressure vessel reach 200 psi.

#### 2.4.4 Pump the Test Fluid to the Test Section

Switch on the “test fluid output” valve on the pressure vessel to let the test fluid flow though the test section before the experiment run. This process is used to remove the air bubble in the test section, so tune the metering valve at the back of the test section to make the flow faster in order to remove the air bubble easily.

#### 2.4.5 Start the Experiment

The experiment measurements are conducted as following:

- i. Turn on the flow meter, Carrier Demodulator, NI data acquisition system, power supply and the computer which connecting the NI system and containing the LabVIEW program.
- ii. Tune the metering valve to control the flow rate of the test fluid in certain Reynolds number. Then tune the power supply to heat up the test section until the temperature difference between the inlet and outlet temperature is continuously in certain level.
- iii. After the experimental condition is stable, which the amplitude of change in flow rate is under 0.01mL/s and that of temperature difference on inlet and outlet is under 0.3°C, run the corresponding program to collect the experimental data. Each data needs to be collected about 1 minute.

## CHAPTER 3: VERIFICATION FOR THE EXPERIMENTAL SETUP

To verify the experimental setup and to compare with the different inlet tube data in the following, the experiments for straight mini-tube were conducted in order to prove its accuracy.

### 3.1 VERIFICATION FOR THE HEAT TRANSFER

The recent mini-tube heat transfer data for the straight inlet which collected by this experimental setup were compared with those of square edged collected by Ghajar and Tam [6]. In this study, the most comment variable to discuss the behavior of heat transfer is the Colburn j factor ( $j=StPr^{0.67}$ ). Figure 3-1 showed the j factors of this study which the range of Reynolds number from 1,000 to 10,000, and the j factors of [6] which the range of Reynolds number from 300 to 40,000. It is reasonable that the difference between the current data and data of [6] is within 20% in the laminar and turbulent regions. However, it can easily see that there was a parallel shift from the classical fully developed value of  $Nu = 4.364$ , the buoyancy effect given a larger mixed convection on the laminar flow [3]. Therefore, in this study, the data was shifted because of the buoyancy effect on laminar flow was more than the square-edged inlet data [6].

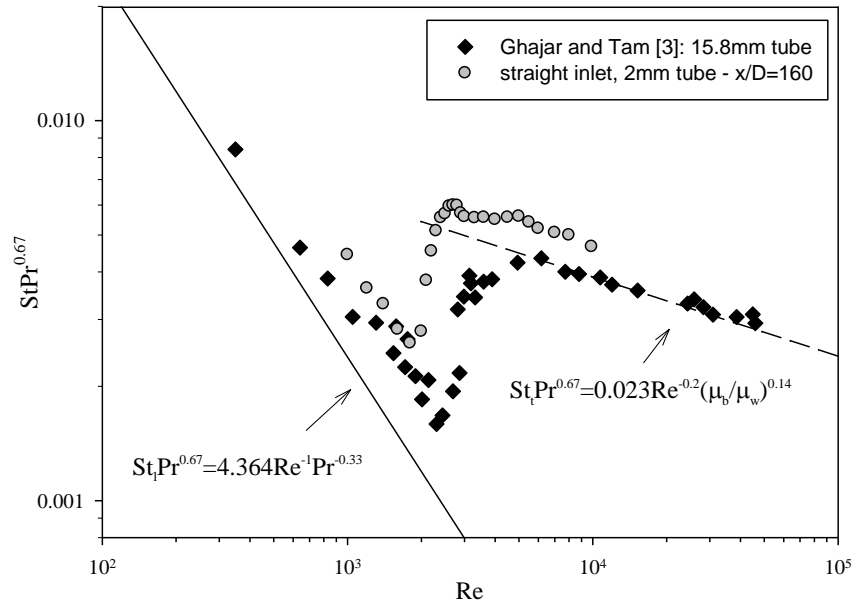


Figure 3-1 Comparison of the present heat transfer data at  $x/D_i$  of 160 with experimental data of [3] at  $x/D_i$  of 200

### 3.2 VERIFICATION FOR THE ISOTHERMAL PRESSURE DROP

The measurements of friction factor collected by this study were verified by comparing with the classical friction factor equations for laminar ( $f = 64/Re$ ) and turbulent flows ( $f = 0.316/Re^{0.25}$ ).

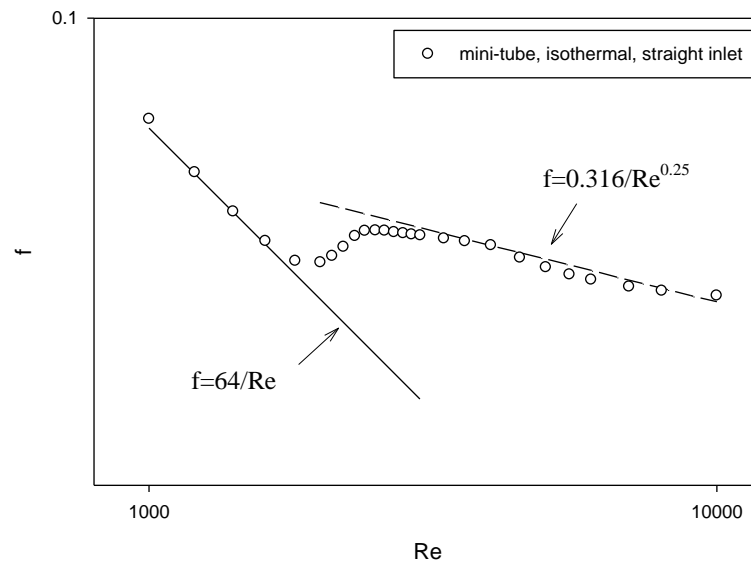


Figure 3-2 Friction factor characteristics for mini-tube under isothermal boundary condition

As shown in Figure 3-2, all the recent friction factor data in laminar and turbulent flow were close (within 5%) with the classical equations for laminar and turbulent flow. It shown the experiment of friction factor data was reliable.

## CHAPTER 4: RESULTS AND DISCUSSION

After verifications of the experimental setup, the heat transfer and pressure drop experiments for the mini-tube in different inlet configurations were conducted. The data results were measured and discussed in the following.

### 4.1 RESULTS OF HEAT TRANSFER

At first, the heat transfer data of the three types of inlet configurations were collected separately in uniform wall heat flux boundary condition. Figure 4-1 to Figure 4-3 shows the Nusselt number of the three inlet configurations in different flow regions, laminar, transition and turbulent flow.

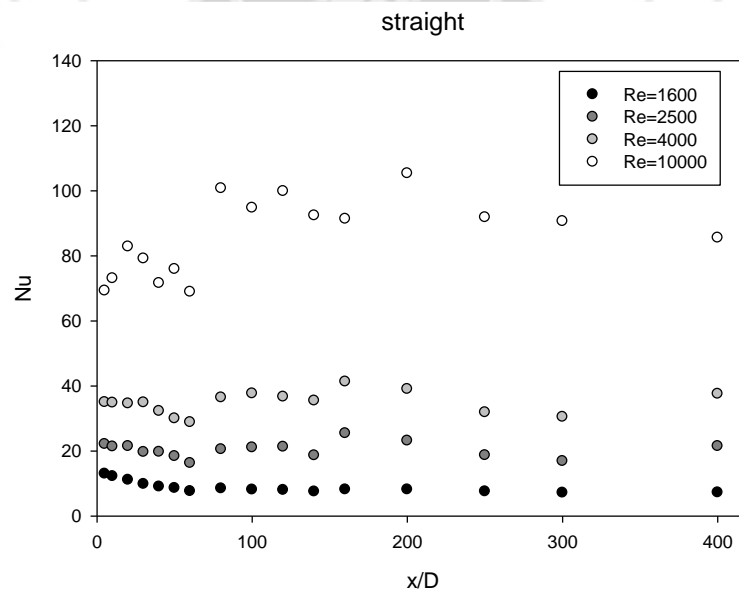


Figure 4-1 Nusselt number for straight inlet in different flow regions

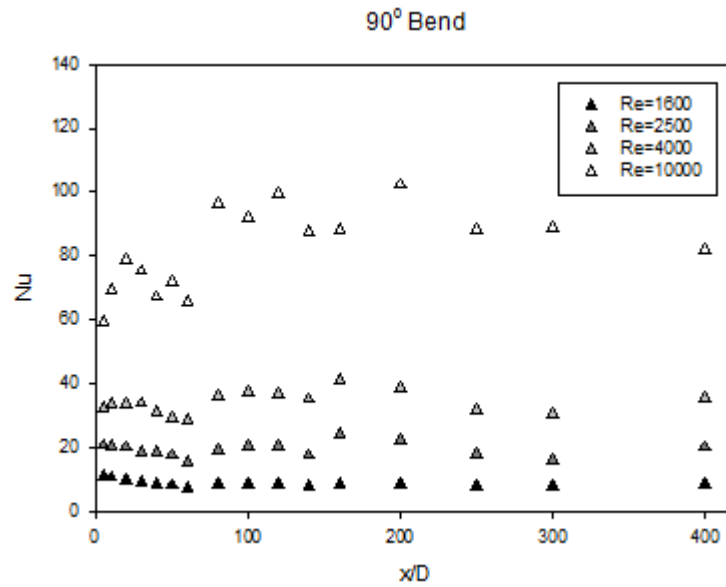


Figure 4-2 Nusselt number for 90° bend inlet in different flow regions

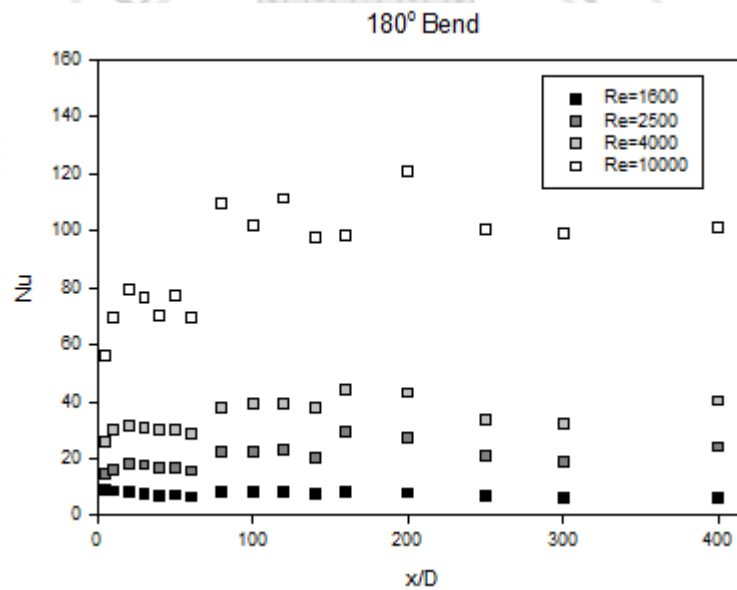


Figure 4-3 Nusselt number for 180° bend inlet in different flow regions

The upper three figures were then combined and discussed in three flow regions; laminar (Figure4-4), transition (Figure4-5) and turbulent (Figure4-6), in order to observe the heat transfer characteristics of different inlet configurations in same flow region.

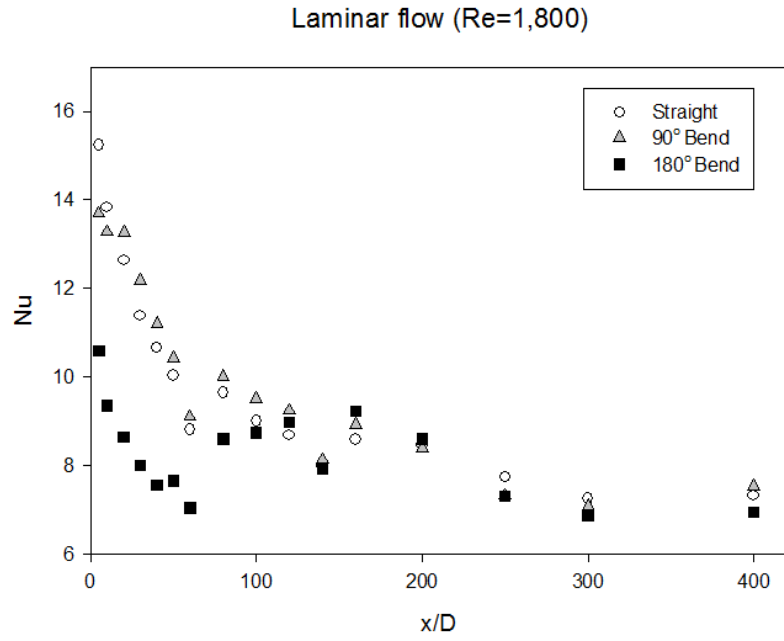


Figure 4-4 Nusselt number for different inlet configurations in laminar flow (Re=1,800)

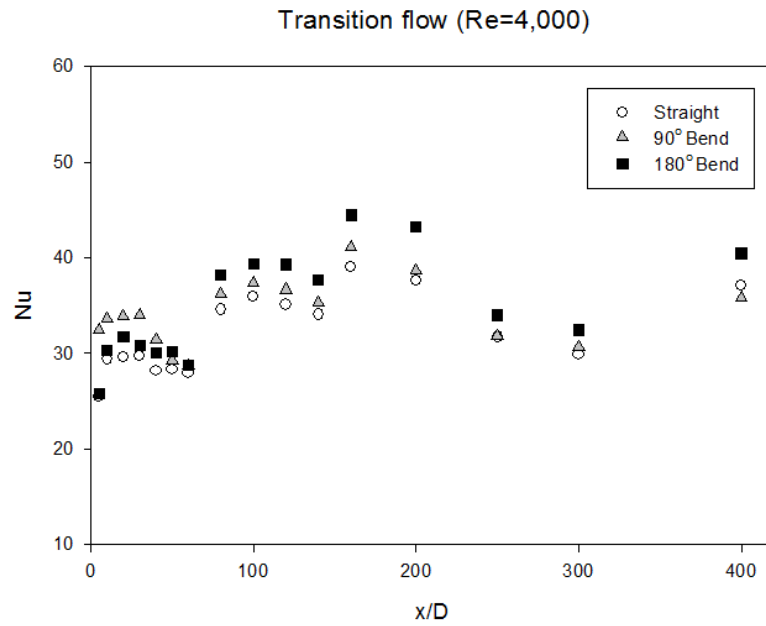


Figure 4-5 Nusselt number for different inlet configurations in transition flow (Re=4,000)



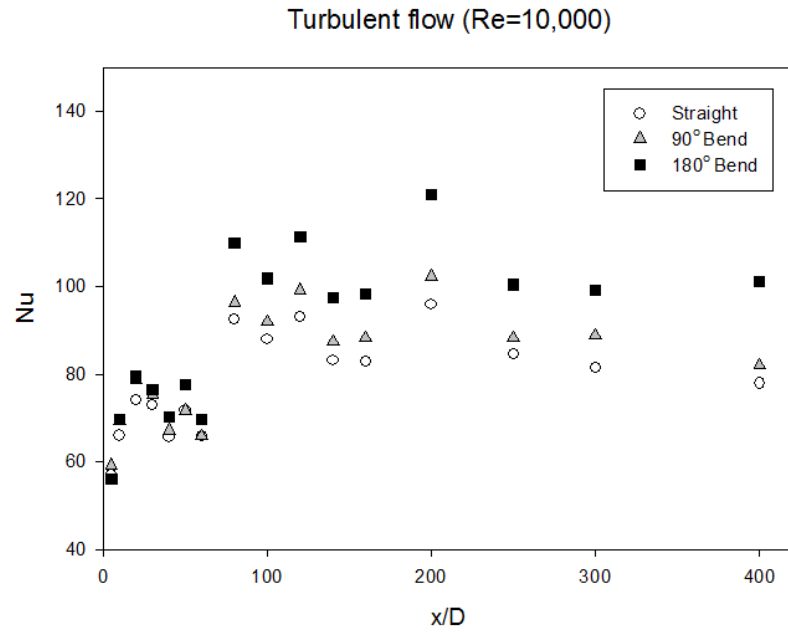


Figure 4-6 Nusselt number for different inlet configurations in turbulent flow ( $Re=10,000$ )

From Figure 4-4, the Nusselt number of  $180^\circ$  bend in developing region is obvious lower than other two inlet configurations before  $x/D_i$  of less than 100. This observation is slightly similar to the bell-mouth effect in transition flow in [2] that the boundary layer along the tube wall is at first laminar and then changes through a transition region to the turbulent condition causing a dip in the  $Nu-x/D_i$  curve, as shown in Figure 4-7.

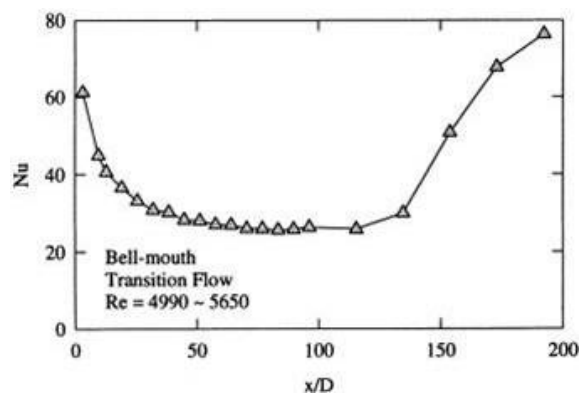


Figure 4-7 Nusselt number arrangement of bell-mouth inlet in transition flow [2]

From Figure 4-5, it shows that 180° bend has slightly higher Nusselt number in transition flow, and the Nusselt number of 90° bend and straight inlet is almost the same. From Figure 4-6, the turbulent flow Nusselt number of 180° bend is obvious the highest and that of 90° bend is slightly higher than that of straight inlet in developed region.

In Figure 4-8, the Colburn j factor value of straight-inlet is obviously greater than the others in turbulent region. Therefore, it can be concluded that the larger bending angle of inlet will increase the heat transfer in a higher flow speed.

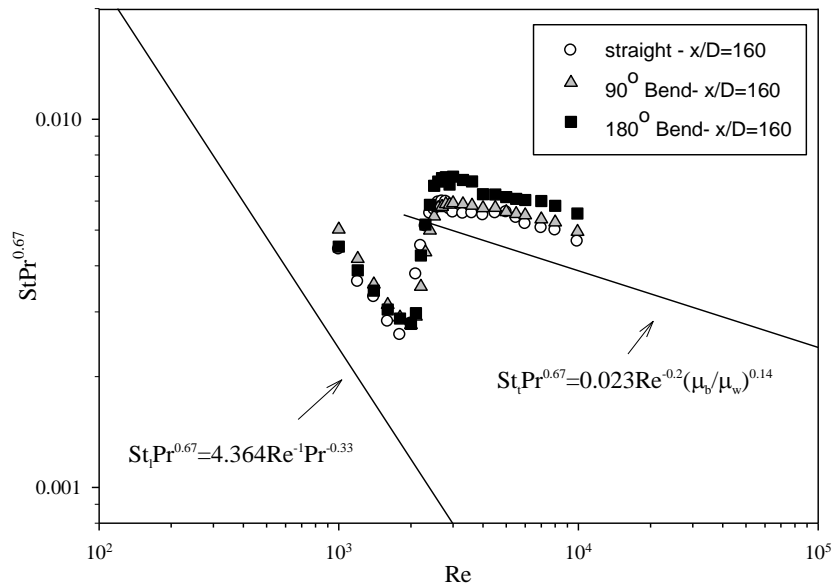


Figure 4-8 Heat transfer characteristics for three different inlet configurations at  $x/D_i = 160$

## 4.2 RESULTS OF ISOTHERMAL FRICTION FACTOR

The result for friction factor is shown in Figures 4-9. As seen in this figure, for mini-tube with three types of inlet configurations under isothermal condition, the start and the end of transition for friction factor were established. The friction factor for the three types of inlet configurations is very similar. It was possibly explained that the experimental setup in this study only collected the pressure difference at the inlet and outlet position to calculate the friction factor.

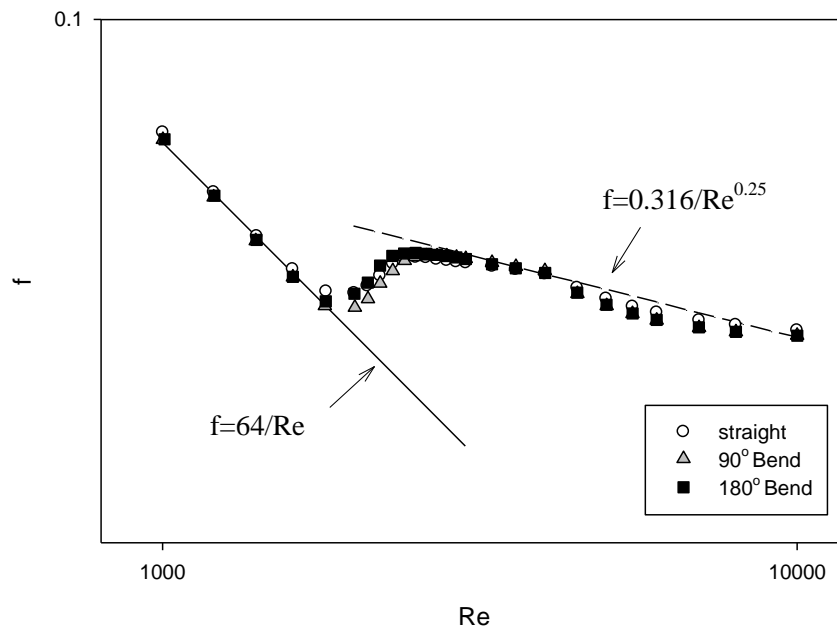


Figure 4-9 Friction factor characteristics for three different inlet configurations under isothermal condition

## CHAPTER 5: CONCLUSIONS

This study could serve as a useful for the design, application and improvement of electro-mechanical equipment, such as HVAC system by the observation of heat transfer and friction factor for mini-tubes in different bending angles. By studying the behavior of smaller tubes, the electro-mechanical equipment can be developed in smaller size in order to increase their application in many different areas.

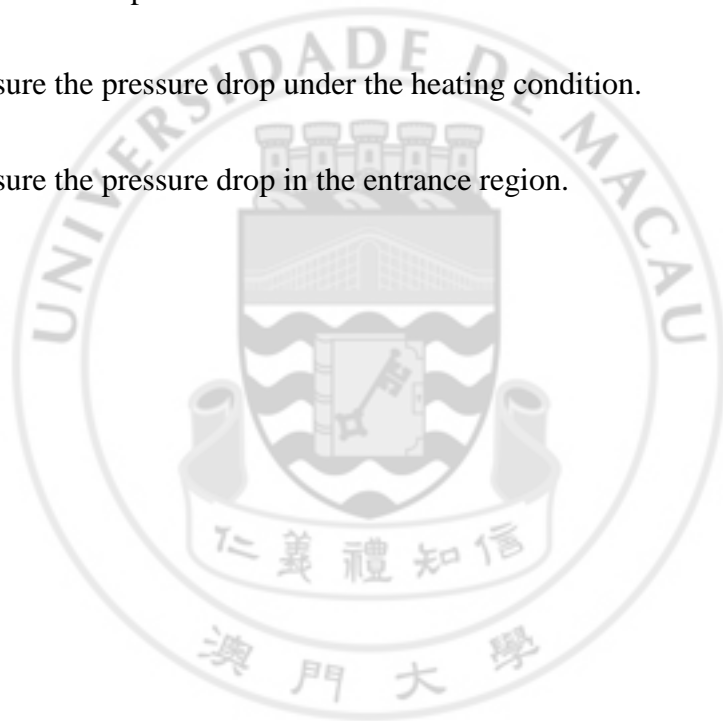
In the experiment of this study, the heat transfer and the friction factor experiments for horizontal mini-tubes with three different inlet configurations (straight, 90° bend and 180° bend) under uniform wall heat flux boundary condition. The experimental data was summarized in the following.

- In the laminar region, 180° bend had a different heat transfer behavior in the developing region than other inlets.
- In the transition and turbulent region, different inlets had the similar heat transfer characteristics. The 180° bend had a higher turbulent heat transfer in the developed region.
- According to the isothermal friction factor results, all the inlets were basically the same from laminar to turbulent region.

## CHAPTER 6: FUTURE WORKS

In this study, a design of an experiment for heat transfer and friction factor in mini-tube with three types of inlet configurations has done. For further study, there are several directions proposed:

- Involve more inlet configurations (e.g.  $45^\circ$  and  $135^\circ$  bends).
- Conduct the experiments with the smaller tube size.
- Measure the pressure drop under the heating condition.
- Measure the pressure drop in the entrance region.



## REFERENCES

- [1] Tam, L. M., Tam, H. K., Ghajar, A. J., Ng, W. S., & Wu, C. K. (2014). The Effect of Inner Surface Roughness and Heating on Friction Factor in Horizontal Mini-tubes. *15th International Heat Transfer Conference*. Kyoto.
- [2] Tam, L. M., & Ghajar, A. J. (1998). The unusual behavior of local heat transfer coefficient in a circular tube with a bell-mouth inlet. *Experimental Thermal and Fluid Science*, 16(3), 187-194.
- [3] Tam, L. M., & Ghajar, A. J. (2006). Transitional Heat Transfer in Plain Horizontal Tubes. *Heat Transfer Engineering*, 27(5), 23-38.
- [4] Boelter, L., Young, G., & Iversen, H. (1948). An Investigation of Aircraft Heaters, XXVII±Distribution of Heat-transfer Rate in the Entrance Section of a Circular Tube. National Advisory Committee for Aeronautics, Technical Note.
- [5] Ghajar, A. J., & Madon, K. F. (1992). Pressure Drop Measurements in the Transition Region for a Circular Tube with Three Different Inlet Configurations. *Experimental Thermal and Fluid Science*, 5, 129-135.
- [6] Ghajar, A. J., & Tam, L. M. (1994). Heat Transfer Measurements and Correlations in the Transition Region for a Circular Tube with Three Different Inlet Configurations. *Experimental Thermal and Fluid Science*, 8, 79-90.
- [7] Ghajar, A. J., & Kim, J. (2006). Calculation of local inside-wall convective heat transfer parameters from measurements of the local outside-wall temperatures along an electrically heated circular tube. In M. Kutz (Ed.), *Heat transfer Calculations* (pp. 23.3-23.27). New York: McGraw-Hill.
- [8] Tam, H. K., Tam, L. M., Ghajar, A. J., Kuok, C. F., & Sun, C. (2015). Experimental Investigation for the Forced and Mixed Convection Heat Transfer inside the Macro- and Mini-tubes. *3rd International Workshop on Heat Transfer Advances for Energy Conservation and Pollution Control*. Taipei.

# APPENDIX (A): DATA OF FIGURE

Data of Figure 4-1

	Nu			
x/D	Re=1600	Re=2500	Re=4000	Re=10000
5	13.00	22.09	35.00	69.28
10	12.22	21.35	34.82	73.05
20	11.10	21.48	34.60	82.83
30	9.83	19.66	34.89	79.15
40	9.01	19.70	32.28	71.57
50	8.57	18.39	29.97	75.91
60	7.62	16.27	28.84	68.90
80	8.45	20.50	36.43	100.73
100	8.10	21.06	37.65	94.75
120	8.00	21.25	36.66	99.86
140	7.52	18.62	35.46	92.40
160	8.16	25.44	41.31	91.36
200	8.13	23.13	39.03	105.34
250	7.56	18.66	31.86	91.81
300	7.15	16.85	30.48	90.61
400	7.23	21.46	37.54	85.54

Data of Figure 4-2

	Nu			
x/D	Re=1600	Re=2500	Re=4000	Re=10000
5	11.18	20.81	32.47	59.23
10	10.91	20.55	33.64	69.26
20	9.95	20.22	33.86	78.67
30	9.20	18.50	34.00	75.39
40	8.67	18.88	31.43	67.17
50	8.39	17.73	29.24	71.73
60	7.65	15.75	28.69	65.84
80	8.84	19.45	36.21	96.31
100	8.73	20.41	37.32	91.90
120	8.72	20.56	36.65	99.21
140	7.89	17.71	35.26	87.51
160	8.90	24.28	41.10	88.33
200	8.69	22.21	38.62	102.24
250	8.00	17.99	31.76	88.36
300	7.82	16.40	30.66	88.76
400	8.59	20.26	35.80	81.98

Data of Figure 4-3

x/D	Nu			
	Re=1600	Re=2500	Re=4000	Re=10000
5	9.01	14.45	25.81	56.04
10	8.82	16.01	30.30	69.76
20	8.15	18.34	31.68	79.46
30	7.56	17.85	30.86	76.39
40	7.15	16.68	30.03	70.25
50	7.29	16.93	30.13	77.54
60	6.72	15.85	28.75	69.58
80	8.16	22.45	38.19	109.98
100	8.25	22.68	39.33	101.83
120	8.44	23.34	39.30	111.41
140	7.53	20.25	37.70	97.51
160	8.64	29.43	44.45	98.38
200	8.10	27.13	43.26	120.92
250	6.87	21.23	33.99	100.40
300	6.50	19.13	32.44	99.11
400	6.40	24.29	40.43	101.15

Data of Figure 4-4

x/D	Nu		
	straight	90° bend	180° bend
5	15.24	13.82	9.52
10	13.83	13.64	9.36
20	12.64	13.04	8.65
30	11.39	12.04	8.01
40	10.67	11.39	7.56
50	10.03	10.69	7.66
60	8.82	9.53	7.05
80	9.65	10.50	8.61
100	9.02	10.04	8.75
120	8.69	9.60	8.99
140	8.00	8.40	7.93
160	8.59	9.22	9.23
200	8.47	8.78	8.61
250	7.75	8.00	7.31
300	7.26	7.76	6.89
400	7.33	8.46	6.74



Data of Figure 4-5

x/D	Nu		
	straight	90° bend	180° bend
5	35.00	32.47	25.81
10	34.82	33.64	30.30
20	34.60	33.86	31.68
30	34.89	34.00	30.86
40	32.28	31.43	30.03
50	29.97	29.24	30.13
60	28.84	28.69	28.75
80	36.43	36.21	38.19
100	37.65	37.32	39.33
120	36.66	36.65	39.30
140	35.46	35.26	37.70
160	41.31	41.10	44.45
200	39.03	38.62	43.26
250	31.86	31.76	33.99
300	30.48	30.66	32.44
400	37.54	35.80	40.43

Data of Figure 4-6

x/D	Nu		
	straight	90° bend	180° bend
5	69.28	59.23	56.04
10	73.05	69.26	69.76
20	82.83	78.67	79.46
30	79.15	75.39	76.39
40	71.57	67.17	70.25
50	75.91	71.73	77.54
60	68.90	65.84	69.58
80	100.73	96.31	109.98
100	94.75	91.90	101.83
120	99.86	99.21	111.41
140	92.40	87.51	97.51
160	91.36	88.33	98.38
200	105.34	102.24	120.92
250	91.81	88.36	100.40
300	90.61	88.76	99.11
400	85.54	81.98	101.15

Data of Figure 4-7

	j factor		
Re	straight	90° bend	180° bend
1000	0.004438	0.005023	0.004511
1200	0.003623	0.004183	0.003889
1400	0.003292	0.003563	0.003423
1600	0.002824	0.003136	0.003042
1800	0.002599	0.002898	0.002875
2000	0.002788	0.002764	0.002780
2100	0.003796	0.002916	0.002975
2200	0.004535	0.003512	0.004266
2300	0.005126	0.004358	0.005177
2400	0.005554	0.004991	0.005857
2500	0.005686	0.005452	0.006596
2600	0.005948	0.005750	0.006774
2700	0.005988	0.005790	0.006922
2800	0.005979	0.005892	0.006961
2900	0.005707	0.005867	0.006649
3000	0.005590	0.005923	0.006990
3300	0.005550	0.005883	0.006845
3600	0.005563	0.005832	0.006783
4000	0.005494	0.005745	0.006261
4500	0.005561	0.005754	0.006249
5000	0.005597	0.005601	0.006146
5500	0.005402	0.005540	0.006083
6000	0.005202	0.005492	0.006036
7000	0.005069	0.005355	0.005998
8000	0.004997	0.005253	0.005821
10000	0.004660	0.004951	0.005546

Data of Figure 4-8

	f		
Re	straight	90° bend	180° bend
1000	0.0664	0.0647	0.0648
1200	0.0535	0.0525	0.0528
1400	0.0456	0.0448	0.0450
1600	0.0404	0.0393	0.0393
1800	0.0373	0.0354	0.0360
2000	0.0371	0.0352	0.0370
2100	0.0381	0.0363	0.0385
2200	0.0395	0.0384	0.0410
2300	0.0412	0.0402	0.0424
2400	0.0421	0.0417	0.0428
2500	0.0422	0.0423	0.0429
2600	0.0421	0.0424	0.0428
2700	0.0419	0.0424	0.0426
2800	0.0417	0.0424	0.0424
2900	0.0415	0.0422	0.0422
3000	0.0414	0.0420	0.0419
3300	0.0408	0.0414	0.0412
3600	0.0404	0.0408	0.0406
4000	0.0397	0.0402	0.0399
4500	0.0378	0.0370	0.0371
5000	0.0363	0.0354	0.0355
5500	0.0353	0.0344	0.0344
6000	0.0345	0.0336	0.0337
7000	0.0336	0.0327	0.0328
8000	0.0330	0.0322	0.0322
10000	0.0324	0.0318	0.0318

## APPENDEX (B): DATA REDUCTION

In this study, LabVIEW was used to collect the data from NI data acquisition device. Before the data was used to analysis the heat transfer condition, calculation has been done in LabVIEW. From [7] heat transfer calculations, the equation of density, viscosity and specific heat were chosen to apply in the experiment.

The following equations were for the thermophysical of water given from [7] and they were originally from Linstrom and Mallard (2003),

$$\text{Density: } \rho_{\text{water}} = 999.96 + 1.7158 \times 10^{-2} T - 5.8699 \times 10^{-3} T^2 + 1.5487 \times 10^{-5} T^3 \quad (\text{B.1})$$

$$\text{Viscosity: } \mu_{\text{water}} = 1.7888 \times 10^{-3} - 5.9458 \times 10^{-5} T + 1.3096 \times 10^{-6} T^2 - 1.8035 \times 10^{-8} T^3 + 1.3446 \times 10^{-10} T^4 - 4.0698 \times 10^{-13} T^5 \quad (\text{B.2})$$

$$\text{Specific heat: } (C_p)_{\text{water}} = 4219.8728 - 3.3863 T + 0.11411 T^2 - 2.1013 \times 10^{-3} T^3 + 2.3529 \times 10^{-5} T^4 - 1.4167 \times 10^{-7} T^5 + 3.58520 \times 10^{-10} T^6 \quad (\text{B.3})$$

where  $T$  is the bulk temperature in the testing tube. Bulk temperature is defined as the average temperature in a testing tube,

$$\text{Bulk Temperature: } T_b = \frac{T_{\text{in}} + T_{\text{out}}}{2} \quad (\text{B.4})$$

therefore, when we get the inlet and outlet temperature, the density, viscosity and specific heat of water can be determined immediately.

After calculating the density, viscosity and specific heat of water, mass flow rate, and Reynolds number can be found out also,

$$\text{Mass flow rate:} \quad M = \rho_{\text{water}} v \pi A \quad (\text{B.5})$$

where  $v$  = velocity of water in the experiment (m/s) and  $A$  = the cross-section area of the pipe. In this experiment, the velocity of water  $v$  was collected by the flow meter. Reynolds number is a ratio of inertial forces and viscous forces in the fluid, it can defined as laminar, transitional and turbulent flows in different Reynolds number.

It is defined as,

$$\text{Reynolds number:} \quad \text{Re} = \rho_{\text{water}} v D / \mu_{\text{water}} \quad (\text{B.6})$$

where  $v$  = velocity of water in the experiment (m/s),  $D$  = diameter of the pipe (m),  $\rho_{\text{water}}$  and  $\mu_{\text{water}}$  are determined from equations (B.1) and (B.2).

By finding out the Reynolds number, friction factor is also an important variable needed to be calculated. Noted that the equation used for determined friction factor in this study is given by pressure loss,

$$\text{Pressure loss:} \quad \Delta P = f \frac{L}{D} \frac{\rho V_{\text{avg}}^2}{2} \quad (\text{B.7})$$

the friction factor is then determined from pressure loss by changing the subject of Eq.

B.7, yielding,

*Friction factor:*

$$f = \frac{2\Delta PD}{\rho L V_{avg}^2} \quad (B.8)$$

where  $\Delta P$  = pressure drop of a fully developed internal flows,  $D$  = diameter of the pipe (m),  $\rho = \rho_{water}$  in this study,  $L$  = length of the test section and  $V_{avg}$  = velocity of water. Noted that  $\Delta P$  is determined by collecting the data from the pressure transducer, which is in Pa.

The total heat transfer between water and the surface of tube is considered as a heat transfer coefficient. However, it might have some loss during the heat exchange process, so here is the equation to determine the loss in the experiment,

$$heat\ balance\ error\ (\%) = \frac{power\ supply - heat\ absorbed}{power\ supply} \times 100\% \quad (B.9)$$

where power supply is defined as power  $P$  supplied by a DC power supply,

*Power:*

$$P = VI \quad (B.10)$$

besides, heat absorbed is defined as the heat transfer between the tube side and the surface of tube,

*Heat absorbed:*

$$\dot{q} = \dot{m} C_p \Delta T \quad (B.11)$$

where  $\dot{m}$  = mass flow rate in Eq. B.5,  $C_p$  = specific heat capacity of water in Eq. B.3 and  $\Delta T$  = temperature difference between the inlet and outlet.

## WORK BREAKDOWN

